

# Properties of some (3+1) dimensional vortex solutions of the $CP^N$ model

L. A. Ferreira <sup>\*</sup>, P. Klimas <sup>\*</sup> and W. J. Zakrzewski <sup>†</sup>

(<sup>\*</sup>) Instituto de Física de São Carlos; IFSC/USP;  
Universidade de São Paulo  
Caixa Postal 369, CEP 13560-970, São Carlos-SP, Brazil

(<sup>†</sup>) Department of Mathematical Sciences,  
University of Durham, Durham DH1 3LE, U.K.

## Abstract

We construct new classes of vortex-like solutions of the  $CP^N$  model in (3+1) dimensions and discuss some of their properties. These solutions are obtained by generalizing to (3+1) dimensions the techniques well established for the two dimensional  $CP^N$  models. We show that as the total energy of these solutions is infinite, they describe evolving vortices and anti-vortices with the energy density of some configurations varying in time. We also make some further observations about the dynamics of these vortices.

# 1 Introduction

In this paper we present new classes of vortex-like solutions of the  $CP^N$  model [1, 2] in (3+1) dimensions. Our results generalize those obtained in our previous paper [3] where we presented a quite large class of exact solutions of  $CP^N$  models in (3 + 1) dimensions. These solutions were described by arbitrary functions of two variables, namely of the combinations  $x^1 + i x^2$  and  $x^3 + x^0$ , where  $x^\mu$ ,  $\mu = 0, 1, 2, 3$  are the Cartesian coordinates of four dimensional Minkowski space-time. Then we considered field configurations, which for fixed values of  $x^3 + x^0$  were holomorphic solutions of the  $CP^N$  model in (2+0) dimensions. The dependence on  $x^3 + x^0$  was assumed to be in terms of phase factors ( $e^{ik(x^3 + x^0)}$ ). These solutions then described straight vortices with waves traveling along them with the speed of light. Solutions of that type were also constructed for an extended version of the Skyrme-Faddeev model [4, 5]. Our previous paper [3] contained other solutions for which the vortices and the waves were in more complicated interactions with each other.

In this paper we generalize the procedure of [3] and generate many more vortex-like solutions and also discuss solutions which correspond to configurations of parallel vortices and anti-vortices. Such structures interact with each other and our solutions describe this interaction and the resultant dynamics. A novelty of the paper is that we generalize to (3 + 1) dimensions a method for constructing solutions which was originally proposed [2] in the context of the two dimensional  $CP^N$  model. Given an holomorphic solution, *i.e.* a configuration depending only on  $x^1 + i x^2$  and  $x^3 + x^0$ , we are able to generate, using a projection operator, solutions depending on  $x^1 + i x^2$ ,  $x^3 + x^0$  and also  $x^1 - i x^2$ .

As our solutions describe vortices their total energy is infinite so to compare various configurations of vortices it is convenient to talk of energy density or energy per unit length. Then, as we discuss in this paper interesting phenomena that can take place - the energy per unit length can stay constant, be periodic in time or even grow with time. At first sight this may seem surprising but, in fact, this is not in contradiction of any principles, as the total energy remains infinite and so is “constant” (*i.e.* does not change). This observation complements the observation of our previous paper [3] in which we pointed out that although the energy per unit length of various parallel vortex configurations can depend on the distance between them the vortices would still remain at rest.

The paper is organized as follows. In the next section, for completeness, we introduce our notation and recall some basic properties of the  $CP^N$  models and of their classical solutions in (2+0) dimensions.

The next section presents our solutions and the following one discusses some properties of these solutions. We finish the paper with a short section presenting our conclusions and further remarks.

## 2 General remarks about the $CP^N$ model

The  $CP^N$  model in  $(3+1)$  dimensional Minkowski space-time is defined in terms of its Lagrangian density

$$\mathcal{L} = M^2(D_\mu \mathcal{Z})^\dagger D^\mu \mathcal{Z}, \quad \mathcal{Z}^\dagger \cdot \mathcal{Z} = 1, \quad (2.1)$$

where  $M^2$  is a constant with the dimension of mass,  $\mathcal{Z} = (\mathcal{Z}_1, \dots, \mathcal{Z}_{N+1}) \in \mathcal{C}^{N+1}$  and it satisfies the constraint  $\mathcal{Z}^\dagger \cdot \mathcal{Z} = 1$ . The covariant derivative  $D_\mu$  acts on any  $N$  component vector  $\Psi$  and so also on  $\mathcal{Z}$ , according to

$$D_\mu \Psi = \partial_\mu \Psi - (\mathcal{Z}^\dagger \cdot \partial_\mu \mathcal{Z}) \Psi.$$

The index  $\mu$  runs here over the set  $\mu = \{0, 1, 2, 3\}$  and the Minkowski metric is  $(+, -, -, -)$ . The Lagrangian (2.1) is invariant under the global transformation  $\mathcal{Z} \rightarrow U \mathcal{Z}$ , with  $U$  being a  $(N+1) \times (N+1)$  unitary matrix. One of the advantages of the  $\mathcal{Z}$  parametrization is that it makes this  $U(N+1)$  symmetry explicit [1, 2]. It is also convenient to use the ‘un-normalized’ vectors  $\hat{\mathcal{Z}}$  with components  $\hat{\mathcal{Z}}_i$ . Then

$$\mathcal{Z} = \frac{\hat{\mathcal{Z}}}{\sqrt{\hat{\mathcal{Z}}^\dagger \cdot \hat{\mathcal{Z}}}}, \quad (2.2)$$

where the dot product involves the summation over all  $(N+1)$  components of  $\hat{\mathcal{Z}}$ .

Sometimes, exploiting the full projective space symmetry of the model, we set  $u = \frac{\hat{\mathcal{Z}}}{\hat{\mathcal{Z}}_{N+1}}$  and so use the parametrization

$$\mathcal{Z} = \frac{(1, u_1, \dots, u_N)}{\sqrt{1 + |u_1|^2 + \dots + |u_N|^2}}. \quad (2.3)$$

The  $u$ -field parametrization does not make the  $U(N+1)$  symmetry explicit but it has the advantage that it brings out the real degrees of the freedom of the model. In terms of  $u_i$ ’s the Lagrangian density (2.1) takes the form

$$\mathcal{L} = \frac{4M^2}{(1 + u^\dagger \cdot u)^2} \left[ (1 + u^\dagger \cdot u) \partial^\mu u^\dagger \cdot \partial_\mu u - (\partial^\mu u^\dagger \cdot u)(u^\dagger \cdot \partial_\mu u) \right]. \quad (2.4)$$

The classical solutions of the model are given by the  $N$  Euler-Lagrange equations which take the form:

$$(1 + u^\dagger \cdot u) \partial^\mu \partial_\mu u_k - 2(u^\dagger \cdot \partial^\mu u) \partial_\mu u_k = 0. \quad (2.5)$$

The simplest  $CP^1$  case is given by one function  $u$ :  $\mathcal{Z} = \frac{(1, u)}{\sqrt{1+|u|^2}}$ .

### 3 Some solutions

In this paper we shall use the notation of [3] *i.e.* we define

$$z \equiv x^1 + i \varepsilon_1 x^2, \quad \bar{z} \equiv x^1 - i \varepsilon_1 x^2, \quad y_\pm \equiv x^3 \pm \varepsilon_2 x^0 \quad (3.6)$$

with  $\varepsilon_a = \pm 1$ ,  $a = 1, 2$ .

It is easy to check that any set of functions  $\hat{Z}_k$  and so  $u_k$  that depend on coordinates  $x^\mu$  in a special way, namely

$$u_k = u_k(z, y_+) \quad (3.7)$$

is a solution of the system of equations (2.5). The Minkowski metric in the coordinates (3.6) becomes  $ds^2 = -dz d\bar{z} - dy_+ dy_-$ . It then follows that (3.7) satisfies simultaneously  $\partial^\mu \partial_\mu u_i = 0$  and  $\partial^\mu u_i \partial_\mu u_j = 0$  for all  $i, j = 1, \dots, N$ . Hence this class of solutions is quite large.

However, these are not the only solutions we can construct very easily. In fact, we can exploit the construction [2] of the solutions of the  $CP^N$  model in (2+0) dimensions (for  $N > 1$ ) to obtain further solutions. To do this we recall the construction in (2+0) dimensions:

First we define a Gramm-Schmidt orthogonalising operator  $P_z$  by its action on any vector  $f \in \mathcal{C}^{N+1}$ , namely

$$P_z f = \partial_z f - f \frac{f^\dagger \cdot \partial_z f}{|f|^2}. \quad (3.8)$$

Then, if we take  $f = f(z)$  and consider  $\hat{Z} = f(z)$  the corresponding  $u$  solves the equations (2.5). Note that as  $f(z)$  does not depend on  $y_\pm$  we have a solution of the  $CP^N$  model in (2+0) and in (3+1) dimensions. However, as is well known, (see *e.g.* [2] and the references therein)

$$\hat{Z} = P_z f(z) \quad (3.9)$$

defines further  $u$ 's which also solve (2.5) in (2+0) dimensions. But, as the expression for  $u$  does not depend on  $y_{\pm}$  these functions also solve the equations (2.5) in (3+1) dimensions. This procedure can then be repeated, namely we can take

$$\hat{Z} = P_z^k f(z), \quad (3.10)$$

where  $P_z^k f = P_z(P_z^{k-1} f)$ .

To have more general solutions we observe that, like in [3], we can make the coefficients of  $z$  in the original  $f(z)$  to be functions of one of  $y_{\pm}$ , say,  $y_+$ . As  $y_+$  is real the operation of applying  $P_z$  operator does not introduce the other  $y_{\pm}$ , *i.e.*  $y_-$ , and so the corresponding  $\hat{Z}$  and so  $u$  give us further solutions of the equations (2.5) in (3+1) dimensions. This way for  $N > 1$  we can have holomorphic solutions and also 'mixed' solutions.

They are given, respectively, by

$$u_k(z, y_+) = \frac{f_k(z, y_+)}{f_{N+1}(z, y_+)} \quad (3.11)$$

and

$$u_k(z, \bar{z}, y_+) \equiv \frac{P_z^l f_k}{P_z f_{N+1}}. \quad (3.12)$$

Note that like in the (2+0) case the last (as we take larger  $l$ ) nonvanishing solution would be antiholomorphic. Then the corresponding  $u_k$  will be functions of only  $\bar{z}$  and  $y_+$ .

### 3.1 Some properties of our solutions

Let us first discuss briefly some quantities which we will use in the discussion of various properties of our solutions.

#### 3.1.1 The energy of the solutions

The Hamiltonian density of the  $CP^N$  model, when written in coordinates  $(z, \bar{z}, y_+, y_-)$ , takes the form

$$\mathcal{H} = \mathcal{H}^{(1)} + \mathcal{H}^{(2)}, \quad (3.13)$$

where

$$\mathcal{H}^{(1)} = \frac{8M^2}{(1 + u^\dagger \cdot u)^2} \left[ \partial_{\bar{z}} u^\dagger \cdot \Delta^2 \cdot \partial_z u + \partial_z u^\dagger \cdot \Delta^2 \cdot \partial_{\bar{z}} u \right] \quad (3.14)$$

$$\mathcal{H}^{(2)} = \frac{8M^2}{(1 + u^\dagger \cdot u)^2} \left[ \partial_+ u^\dagger \cdot \Delta^2 \cdot \partial_+ u + \partial_- u^\dagger \cdot \Delta^2 \cdot \partial_- u \right] \quad (3.15)$$

and  $\Delta_{ij}^2 \equiv (1 + u^\dagger \cdot u)\delta_{ij} - u_i u_j^*$ .

For solutions depending on  $y_+$  *i.e.* described by  $u_k(z, \bar{z}, y_+)$  the part of the Hamiltonian density (3.15) that contains  $\partial_-$  drops out. For the holomorphic solutions the second part of (3.14) also drops out. For the ‘mixed’ solutions described by (3.12) both parts of (3.14) are nonzero.

Note that as our solutions depend on variables  $x^0$  and  $x^3$  only through the combination  $y_+$  it is useful to define the concept of energy per unit length which involves the integration over  $x^1$  and  $x^2$  (*i.e.* over the plane perpendicular to the  $x^3$  axis). This gives us

$$\mathcal{E} = \int_{R^2} dx^1 dx^2 \mathcal{H} = 8\pi M^2 \left[ \mathcal{I}^{(1)} + \mathcal{I}^{(2)} \right],$$

where

$$\mathcal{I}^{(a)} \equiv \frac{1}{8\pi M^2} \int_{R^2} dx^1 dx^2 \mathcal{H}^{(a)}, \quad a = 1, 2.$$

### 3.1.2 The topological charge

As we are working with vortex configurations it is important to introduce the two-dimensional topological charge defined by the integral

$$Q_{\text{top}} = \int_{R^2} dx^1 dx^2 \rho_{\text{top}} \quad (3.16)$$

whose density is given by

$$\begin{aligned} \rho_{\text{top}} &= \frac{1}{\pi} \varepsilon_{ij} (D_i \mathcal{Z})^\dagger \cdot (D_j \mathcal{Z}) = \frac{1}{\pi} \varepsilon_{ij} \frac{\partial_i u^\dagger \cdot \Delta^2 \cdot \partial_j u}{(1 + u^\dagger \cdot u)^2} = \\ &= \frac{1}{\pi} \frac{\partial_{\bar{z}} u^\dagger \cdot \Delta^2 \cdot \partial_z u - \partial_z u^\dagger \cdot \Delta^2 \cdot \partial_{\bar{z}} u}{(1 + u^\dagger \cdot u)^2}. \end{aligned} \quad (3.17)$$

The indices  $i$  and  $j$  here only take two values  $\{1, 2\}$ . It is easy to see that for the holomorphic solution  $Q_{\text{top}} = \mathcal{I}^{(1)}$ .

## 4 Vortex solutions of the $CP^N$ model and some of their properties

In [3] we studied some general classes of solutions of the  $CP^1$  model. Here, first of all, we concentrate our attention on two classes of holomorphic solutions of the  $CP^1$  model and then look in some detail at the  $CP^2$  model concentrating our attention this time on ‘mixed’ solutions (3.12).

### 4.1 $CP^1$ solutions

In the  $CP^1$  model we have two functions  $f_1$  and  $f_2$  and in our discussion we can take their ratio  $u = \frac{f_1}{f_2}$ .

Let us first consider the case when all the dependence on  $y_+$  is in the form of phase factors  $e^{ik_i y_+}$  where  $k_i$  are constant. Many interesting features are observed for the configurations given by

$$f_1(z, y_+) = z^2 + a_1 z e^{ik_1 y_+}, \quad f_2(z, y_+) = a_2 z + a_3 e^{ik_2 y_+}, \quad (4.18)$$

where we have assumed, for simplicity, that all three parameters  $a_1$ ,  $a_2$  and  $a_3$  are real. The generalization to their complex values does not bring anything new to the problem.

The holomorphic solution  $u$  is then of the form

$$u(z, y_+) = z \frac{z + a_1 e^{ik_1 y_+}}{a_2 z + a_3 e^{ik_2 y_+}}. \quad (4.19)$$

The zeros of denominator do not lead to the singularities in the energy density as both integrals  $\mathcal{I}^{(1)}$  and  $\mathcal{I}^{(2)}$  are invariant with respect to the inversion  $u \rightarrow \frac{1}{u}$ .

Next we look in detail at various special cases of this solution (4.19).

#### 4.1.1 The tube solution

First we consider the case of  $a_1 = a_2 = 0$ . In this case the field configuration becomes

$$u = \frac{z^2}{a_3} e^{-ik_2 y_+}. \quad (4.20)$$

It is easy to convince oneself that this field configuration describes a vortex with waves traveling along it with the speed of light. The profile of the energy

density is independent of  $y_+$ . It has a maximum at a ring of radius  $r_0$  which satisfies  $r_1 < r_0 < r_2$ , where  $r_1 = \sqrt{\frac{|a_3|}{\sqrt{3}}}$  is the radius of the circle at which the Hamiltonian density  $\mathcal{H}^{(1)}$  has a maximum, and  $r_2 = \sqrt{|a_3|}$  corresponds to the radius of the circle at which  $\mathcal{H}^{(2)}$  has a maximum. The radius  $r_0$  depends on  $a_3$  and  $k_2$ . For  $k_2 \rightarrow 0$  it tends to  $r_1$  and for  $k_2 \rightarrow \pm\infty$  it tends to  $r_2$ . The integral  $\mathcal{I}^{(1)}$  describes the topological charge of the vortex which for the solution considered here is

$$\mathcal{I}^{(1)} = \frac{1}{\pi} \int_{R^2} dx^1 dx^2 \frac{4a_3^2 |z|^2}{(a_3^2 + |z|^4)^2} = 2.$$

The contribution to the energy per unit length that comes from the traveling waves can be also calculated explicitly. We find

$$\mathcal{I}^{(2)} = \frac{1}{\pi} \int_{R^2} dx^1 dx^2 k_2^2 \frac{a_3^2 |z|^4}{(a_3^2 + |z|^4)^2} = \frac{\pi}{4} k_2^2 |a_3|.$$

A modification of a solution of this type had been already studied in [3]. An example of such a solution is shown in Fig 1, where we plot the components of the isovector

$$\vec{n} = \frac{1}{1 + |u|^2} (u + u^*, -i(u - u^*), |u|^2 - 1) \quad (4.21)$$

which depend on  $y_+$ . As  $y_+$  changes the images in Fig.1 rotate. In Fig. 2, we plot the two contributions, topological and wave, of the energy density on the solution (4.20).

#### 4.1.2 The spiral solution

A less trivial but still a very simple solution is obtained from (4.19) by putting  $a_3 = 0$ , and so  $u$  is given by

$$u = \frac{1}{a_2} (z + a_1 e^{ik_1 y_+}). \quad (4.22)$$

In this case the integrals  $\mathcal{I}^{(1)}$  and  $\mathcal{I}^{(2)}$  can be calculated explicitly. They take the values

$$\mathcal{I}^{(1)} = \frac{1}{\pi} \int_{R^2} dx^1 dx^2 \frac{1}{a_2^2 (1 + |u|^2)^2} = 1, \quad (4.23)$$

$$\mathcal{I}^{(2)} = \frac{1}{\pi} \int_{R^2} dx^1 dx^2 \frac{1}{a_2^2 (1 + |u|^2)^2} a_1^2 k_1^2 = a_1^2 k_1^2. \quad (4.24)$$



In Fig. 3 we plot the components of the isovector (4.21) for the solution (4.22). In order to analyze the energy density let us introduce the parameterization  $z = re^{i\varphi}$ . Then

$$|u|^2 = \frac{1}{a_2^2} \left[ r^2 + a_1^2 - 2a_1r \cos(\varphi - k_1y_+ - \pi) \right]$$

We note that the energy per unit length ( $\mathcal{H}$  integrated over the  $x^1 x^2$  plane) does not depend on  $a_2$  or  $y_+$ , whereas the energy density  $\mathcal{H}$  does. The maximum of the energy density ( $|u|^2 = 0$ ) is located at  $r = |a_1|$  and  $\varphi = k_1y_+ + \pi$ . The curve  $(a_1 \cos(k_1y_+ + \pi), a_1 \sin(k_1y_+ + \pi), y_+)$  that joins the points at which the energy density has a local maximum is a spiral. On this spiral not only  $\mathcal{H}$  has a maximum but so do also both its contributions  $\mathcal{H}^{(1)}$  and  $\mathcal{H}^{(2)}$ . As  $y_+ = x^3 + x^0$ , we note that the spiral rotates around the  $x^3$  axis with the speed of light. The only effect of the dependence on  $y_+$  is the rotation of the energy density. Thus the energy per unit length calculated for e.g.  $y_+ = 0$  is also valid for other values of the variable  $y_+$ .

#### 4.1.3 The general case (4.19)

For general values of  $a_1$ ,  $a_2$  and  $a_3$  the expressions for the contributions to the energy become rather complicated. We can write them as

$$\mathcal{I}^{(1)} = \frac{1}{\pi} \int_{R^2} dx^1 dx^2 \frac{A}{C^2}, \quad \mathcal{I}^{(2)} = \frac{1}{\pi} \int_{R^2} dx^1 dx^2 \frac{B}{C^2}, \quad (4.25)$$

where the expressions for  $A$ ,  $B$  and  $C$  take the form (written in cylindrical coordinates  $(r, \varphi, y_+)$  with  $z = re^{i\varphi}$ )

$$\begin{aligned} A &= a_1^2 a_3^2 + 4a_3^2 r^2 + a_2^2 r^4 + 2a_1 a_2 a_3 r^2 \cos[2\varphi - (k_1 + k_2)y_+] \\ &+ 4a_1 a_3^2 r \cos(\varphi - k_1 y_+) + 4a_2 a_3 r^3 \cos(\varphi - k_2 y_+) \end{aligned} \quad (4.26)$$

$$\begin{aligned} B &= r^2 a_1^2 a_3^2 (k_1 - k_2)^2 + r^4 (a_1^2 a_2^2 k_1^2 + a_3^2 k_2^2) \\ &- 2a_1 a_3^2 (k_1 - k_2) k_2 r^3 \cos[\varphi - k_1 y_+] \\ &+ 2a_1^2 a_2 a_3 (k_1 - k_2) k_1 r^3 \cos[\varphi - k_2 y_+] \\ &- 2a_1 a_2 a_3 k_1 k_2 r^4 \cos[(k_1 - k_2)y_+] \end{aligned} \quad (4.27)$$

$$\begin{aligned} C &= r^2 \left[ r^2 + 2a_1 r \cos[\varphi - k_1 y_+] + a_1^2 \right] \\ &+ a_2^2 \left[ r^2 + 2\frac{a_3}{a_2} r \cos[\varphi - k_2 y_+] + \left(\frac{a_3}{a_2}\right)^2 \right]. \end{aligned} \quad (4.28)$$

To fully analyse these expressions requires numerical work. In Figs. 5 and 6 we present the plots of the isovector (4.21) as well as of the energy densities for a

particular example of the above solution. However, even for a general configuration, it is possible to make a few analytical observations:

- Rotations:

Note that the energy per unit length depends on  $y_+$  through periodic functions, involving four frequencies, namely  $k_1$ ,  $k_2$  and  $k_1 \pm k_2$ . However, one can isolate four situations where only one frequency is relevant and the time evolution reduces to a rotation around the  $x^3$ -axis. In such cases,  $A$ ,  $B$  and  $C$  depend on  $\varphi$  and  $y_+$  only through the combination  $\varphi - \omega y_+$ , and the four possibilities when this happens are:

1.  $k_1 = k_2 \equiv k$  and  $\omega = k$
2.  $a_1 = 0$  and  $\omega = k_2$
3.  $a_2 = 0$  and  $\omega = k_1$
4.  $a_3 = 0$  and  $\omega = k_1$

Note that the spiral solution (4.22) belongs to the last case and the tube solution (4.20) corresponds to the case when none of the frequencies matters.

- Singularity

The solution (4.19) exhibits an interesting property when  $a_1 = \frac{a_3}{a_2}$ . Indeed, in this case it reduces to  $u = z/a_2$  whenever  $(k_2 - k_1)y_+ = 2\pi n$ , with  $n$  integer. The case  $k_1 = k_2$  is not interesting since it leads to a solution independent of  $y_+$ . However, for  $k_1 \neq k_2$  the solutions change their properties, including the two dimensional topological charge (3.16), whenever  $y_+ = \xi_n \equiv \frac{2\pi n}{k_2 - k_1}$ . For those special values of  $y_+$  the quantities (4.26)-(4.27) become

$$A = a_2^2 |\vec{r} - \vec{r}_n|^4, \quad B = a_3^2 (k_1 - k_2)^2 r^2 |\vec{r} - \vec{r}_n|^2, \quad C = (r^2 + a_2^2) |\vec{r} - \vec{r}_n|^2$$

where  $\vec{r}$  and  $\vec{r}_n$  are two-component vectors:  $\vec{r} \rightarrow (x, y)$ , and  $\vec{r}_n \rightarrow (x_n, y_n)$ , with

$$x_n = \frac{a_3}{a_2} \cos(k_1 \xi_n + \pi), \quad y_n = \frac{a_3}{a_2} \sin(k_1 \xi_n + \pi). \quad (4.29)$$

The expression  $|\vec{r} - \vec{r}_n|^2$  then becomes

$$\begin{aligned} |\vec{r} - \vec{r}_n|^2 &= (x - x_n)^2 + (y - y_n)^2 \\ &= r^2 - 2 \frac{a_3}{a_2} r \cos(\varphi - k_1 \xi_n - \pi) + \left(\frac{a_3}{a_2}\right)^2. \end{aligned} \quad (4.30)$$

The cancellation changes the degree of polynomials of variable  $z$  which causes the topological charge to jump from  $Q_{\text{top}} = 2$  down to  $Q_{\text{top}} = 1$ . The new topological charge is then given by the integral  $\mathcal{I}^{(1)}$

$$Q_{\text{top}} \equiv \mathcal{I}^{(1)} = \frac{1}{\pi} \int_{R^2} dx^1 dx^2 \frac{a_2^2}{(r^2 + a_2^2)^2} = 1. \quad (4.31)$$

Of course, such behaviour is well known from the study of topological solitons [6]. The space of parameters of the field configuration is not complete (has ‘holes’) and the integrand of the charge density has corresponding delta functions, which are not seen in (4.31). The interesting property here is that this process of the vortex shrinking to the delta function and then expanding again is a function of time; *i.e.* is part of the dynamics of the system and is described by our solution.

The second and related important fact comes from the study of the integral  $\mathcal{I}^{(2)}$ . One can check that when the vortex shrinks to the delta function (*i.e.* the cancellation takes place) the integral

$$\mathcal{I}^{(2)} = \frac{1}{\pi} \int_{R^2} dx^1 dx^2 \frac{a_3^2 (k_1 - k_2)^2 r^2}{(r^2 + a_2^2)^2 |\vec{r} - \vec{r}_n|^2} \quad (4.32)$$

diverges. This divergence comes from the singularity at the point  $\vec{r} = \vec{r}_n$  which is responsible for the energy of the solution becoming infinite. Clearly, from a physical point of view such field configurations should be excluded.

- Anti-holomorphic solutions

We can now also apply the transformation (3.8) to (4.19) and this would give us an anti-holomorphic solution. Its properties are not very different from what we had for the holomorphic one (except that the choice and meaning of parameters is different) so we do not discuss it here.

#### 4.1.4 Further Comments

In our discussion so far we have assumed that all  $y_+$  dependence of the 2-dimensional  $u(z)$  is of the form of phase factors  $\exp(iky_+)$ ’s. There is, of course, no need to be so restrictive. We could make the parameters of the 2-dimensional  $u(z)$  depend on  $y_+$  in a more general way. Thus we could consider, for instance, also

$$u(z, y_+) = \lambda \frac{1}{z - a(y_+)}, \quad (4.33)$$

where  $a(y_+)$  is an arbitrary function.

Then, taking *e.g.*  $a(y_+) = ay_+$  would result in a vortex located at  $x^2 = 0$ ,  $x^1 = ax^3$  moving in the  $x^3$  direction with the velocity of light. Taking a more complicated function, *e.g.*  $a(y_+) = ay_+^2$  would result in a curved vortex  $x^1 = a(x^3)^2$  etc. One can also combine this dependence, for systems of more vortices, with the other dependences discussed above. This complicates the discussion but does not change its main features, hence in the remainder of this paper we return to the discussion of the dependence on  $y_+$  through the phase factors.

One could naively think that infiniteness of the total energy of our solution is related to some “improper” choice of the dependence on  $y_+$ . This is not true since the origin of the divergence comes from the topological nature of  $\mathcal{H}^{(1)}$ . The fact that  $\mathcal{H}^{(1)}$  is a total derivative prevents the dependence of  $\mathcal{H}^{(1)}$  on any parameters (including any depending on  $y_+$ ). One can note that for some special cases like  $u = z^2 \exp(-ay_+^2)$  the contribution to the total energy coming from  $\mathcal{H}^{(2)}$  is finite but the total energy remains infinite since  $\mathcal{H}^{(1)}$  contribution is always present.

## 4.2 The $CP^2$ model

Next we consider solutions of the  $CP^2$  model. First we look at the holomorphic ones.

### 4.2.1 The holomorphic solutions

The simplest  $CP^2$  model solution can be obtained by adding to the system (4.18) a constant third function, *i.e.* define

$$\begin{aligned} f_1(z, y_+) &= z^2 + a_1 z e^{ik_1 y_+} \\ f_2(z, y_+) &= a_2 z + a_3 e^{ik_2 y_+} \\ f_3(z, y_+) &= a_4. \end{aligned} \quad (4.34)$$

Then we can define holomorphic configurations as  $u_i = \frac{f_i}{f_3}$ ,  $i = 1, 2$ , *i.e.*

$$u_1(z, y_+) = \frac{z^2 + a_1 z e^{ik_1 y_+}}{a_4}, \quad u_2(z, y_+) = \frac{a_2 z + a_3 e^{ik_2 y_+}}{a_4}. \quad (4.35)$$

Alternatively, we can interchange  $f_2 \leftrightarrow f_3$  and consider the holomorphic configurations

$$\tilde{u}_1(z, y_+) = \frac{z^2 + a_1 z e^{ik_1 y_+}}{a_2 z + a_3 e^{ik_2 y_+}}, \quad \tilde{u}_2(z, y_+) = \frac{a_4}{a_2 z + a_3 e^{ik_2 y_+}}. \quad (4.36)$$

Note from (2.3) that such an interchange corresponds to a phase transformation in  $\mathcal{Z}$ , so both configurations describe the same solution of the  $CP^2$  model. Note also (easier from (4.36)) that when  $a_4 \rightarrow 0$  this  $CP^2$  solution reduces to the holomorphic  $CP^1$  solution discussed before. In fact,  $\tilde{u}_2$  vanishes, and  $\tilde{u}_1$  becomes the  $CP^1$   $u$ -field.

The integrals  $\mathcal{I}^{(1)}$ ,  $\mathcal{I}^{(2)}$  for this  $CP^2$  holomorphic solution (using definition (4.35) or (4.36)) now take the form

$$\mathcal{I}^{(1)} = \frac{1}{\pi} \int_{R^2} dx^1 dx^2 \frac{\mathcal{A}}{\mathcal{C}^2}, \quad \mathcal{I}^{(2)} = \frac{1}{\pi} \int_{R^2} dx^1 dx^2 \frac{\mathcal{B}}{\mathcal{C}^2} \quad (4.37)$$

where  $\mathcal{A}$ ,  $\mathcal{B}$ ,  $\mathcal{C}$  differ from  $A$ ,  $B$ ,  $C$  given by (4.26), (4.27) and (4.28) by terms proportional to  $a_4^2$ , *i.e.*

$$\mathcal{A} = A + a_4^2 [a_1^2 + a_2^2 + 4r^2 + 4a_1 r \cos(\varphi - k_1 y_+)] \quad (4.38)$$

$$\mathcal{B} = B + a_4^2 [a_1^2 k_1^2 r^2 + a_3^2 k_2^2] \quad (4.39)$$

$$\mathcal{C} = C + a_4^2. \quad (4.40)$$

The Hamiltonian density  $\mathcal{H}^{(2)}$ , which is proportional to  $\frac{\mathcal{B}}{\mathcal{C}^2}$ , is now regular at  $\vec{r} = \vec{r}_n$  and  $y_+ = \xi_n$  for  $a_1 = \frac{a_3}{a_2}$  (where previously we had a singularity) as now it takes the value

$$\frac{\mathcal{B}}{\mathcal{C}^2} \Big|_{\vec{r}=\vec{r}_n, y_+=\xi_n} = \frac{a_3^2}{a_4^2} \left[ \frac{a_3^2}{a_2^4} k_1^2 + k_2^2 \right].$$

Hence we note that going to the  $CP^2$  manifold (by taking  $a_4 \neq 0$ ) has ‘filled in the hole’ in the space of parameters (*i.e.* as the system evolves none of its vortices shrinks to the delta function).

Note also that the energy density is independent of  $y_+$  in four cases:  $k_1 = k_2$ ,  $a_1 = 0$ ,  $a_2 = 0$  and  $a_3 = 0$ .

#### 4.2.2 The mixed solution

Next we look at the ‘new’ mixed solutions. First we use (3.8) to calculate  $P_z f$ . We find that for the system (4.34) they take the form

$$\begin{aligned} P_z f_1 &= a_4^2 e^{ik_1 y_+} \left[ 2z e^{-ik_1 y_+} + a_1 \right] \\ &\quad + e^{ik_1 y_+} \left[ a_3 + a_2 \bar{z} e^{ik_2 y_+} \right] \left[ a_1 a_3 + 2a_3 z e^{-ik_1 y_+} + a_2 z^2 e^{-i(k_1+k_2)y_+} \right] \\ P_z f_2 &= a_2 a_4^2 \end{aligned}$$

$$\begin{aligned}
& - e^{ik_2 y_+} \bar{z} \left[ a_1 + \bar{z} e^{ik_1 y_+} \right] \left[ a_1 a_3 + 2a_3 z e^{-ik_1 y_+} + a_2 z^2 e^{-i(k_1+k_2)y_+} \right] \\
P_z f_3 & = -a_4 e^{-ik_2 y_+} \left[ a_2 a_3 + a_2^2 \bar{z} e^{ik_2 y_+} + \bar{z} e^{ik_2 y_+} (\bar{z} e^{ik_1 y_+} + a_1) (2z e^{-ik_1 y_+} + a_1) \right]
\end{aligned}$$

When written in terms of  $u_i$  this mixed solution is given by

$$u_1(z, \bar{z}, y_+) = \frac{P_z f_1}{P_z f_3}, \quad u_2(z, \bar{z}, y_+) = \frac{P_z f_2}{P_z f_3}. \quad (4.41)$$

Note that in the limit  $a_4 \rightarrow 0$  the mixed solution (4.41) becomes the anti-holomorphic solution of the  $CP^1$  model mentioned before. However for  $a_4 \neq 0$  the solution is different. This time the expressions for the energy density are quite complicated - so we do not present them here. However, we note that to guarantee the convergence of the integral  $\mathcal{I}^{(2)}$  we have to require that  $a_2 \neq 0$ .

To demonstrate that the energy per unit length does not depend on  $y_+$  can be checked without much effort. First, we observe that the overall factors  $e^{ik_j y_+}$  in  $P_z f_k$  do not matter as they cancel in the expressions for  $|u_j|^2$  and for  $|\Delta \cdot u_j|^2$ . Hence, the only relevant expressions are of the form  $z e^{-ik_j y_+} = r e^{i(\varphi - k_j y_+)}$  and  $\bar{z} e^{ik_j y_+} = r e^{-i(\varphi - k_j y_+)}$ . When  $k_1 = k_2 \equiv k$  the energy density depends only on the combination  $(\varphi - k y_+)$  and  $r$  showing that the only effect of the dependence on time is a rotation and, in consequence, the independence of the energy per unit length on  $y_+$  (or  $x^0$  for given  $x^3$ ). The other cases guaranteeing this are  $a_1 = 0$  and  $a_3 = 0$ .

### 4.2.3 The anti-holomorphic solution

Finally we look at the corresponding anti-holomorphic solution. Such a solution derived from the system (4.34) takes the form

$$u_1(\bar{z}, y_+) = \frac{P_z^2 f_1}{P_z^2 f_3} = \frac{a_2 a_4 e^{i(k_1+k_2)y_+}}{a_1 a_3 + \bar{z} e^{ik_1 y_+} (2a_3 + a_2 \bar{z} e^{ik_2 y_+})} \quad (4.42)$$

$$u_2(\bar{z}, y_+) = \frac{P_z^2 f_2}{P_z^2 f_3} = -\frac{a_4 e^{ik_2 y_+} (a_1 + 2\bar{z} e^{ik_1 y_+})}{a_1 a_3 + \bar{z} e^{ik_1 y_+} (2a_3 + a_2 \bar{z} e^{ik_2 y_+})}. \quad (4.43)$$

Note that, like for the ‘mixed case’, we have to require that  $a_2 \neq 0$  as otherwise

$$\mathcal{H}^{(1)} = 0, \quad \mathcal{H}^{(2)} = 8\pi M^2 \frac{k_2^2 a_3^2 a_4^2}{(a_3^2 + a_4^2)^2}.$$

In the next subsection we will produce an explicit example of these field configurations and discuss some of their properties. To avoid the problems mentioned

above our example will have  $a_2 \neq 0$ . Note that in such a case the conditions of the independence of the energy per unit length on  $y_+$  are the same as for the mixed solution.

#### 4.2.4 An example

In our example we start with the set of functions (4.34) for which we have chosen the following values of parameters:  $a_1 = 2.5$ ,  $a_2 = 0.6$ ,  $a_3 = 1.0$ ,  $a_4 = 0.01$ ,  $k_1 = 1.0$  and  $k_2 = 2.0$ . The topological charge of the holomorphic solution is then  $Q_{\text{top}} = 2$ . The topological charge density at  $x^0 = 0$  (and for  $x^3 = 0$ ) has two peaks - one of them is localized at  $z = 0$ , the other a bit further out - see Fig. 7. For the holomorphic solution the topological charge density is proportional to the energy density and this leads to the energy per unit length being given by  $8\pi M^2 \mathcal{I}^{(1)}$ . The integrand  $\mathcal{H}^{(1)}/8M^2$  is sketched in Fig. 8. The contribution coming from the waves  $\mathcal{H}^{(2)}/8M^2$  is plotted in Fig. 9. The mixed solution generated by the application of the  $P_z$  operator according to (3.8) leads to a solution which has  $Q_{\text{top}} = 2 - 2 = 0$  and  $\mathcal{I}^{(1)} = 2 + 2 = 4$ . As is easy to see from Fig. 7 the application of  $P_z$  has changed two holomorphic peaks into two anti-peaks and in addition it has generated two new peaks. The energy density  $\mathcal{H}^{(1)}$  thus has four peaks and  $\mathcal{H}^{(2)}$  only three (with the zero in the place of the fourth  $\mathcal{H}^{(1)}$  one).

The next application of the  $P_z$  operator changes two peaks of the topological charge density into two anti-peaks and annihilates the previous anti-peaks. Thus the anti-holomorphic solution is characterized by  $Q_{\text{top}} = -2$  and  $\mathcal{I}^{(1)} = 2$ . The contribution to the energy per unit length  $8M^2 \mathcal{I}^{(1)}$  is the same as for the initial (holomorphic) case. Nevertheless, the total energies per unit length for these two solutions differ since for solutions of the  $CP^2$  model the integrals  $\mathcal{I}^{(2)}$  are different ( $\mathcal{I}_{\text{hol}}^{(2)} \neq \mathcal{I}_{\text{anti-hol}}^{(2)}$ ). Let us note that our case has a time-dependent energy per unit length (calculated by the integration over the  $x^1 x^2$  plane). It implies that the dependence of the energy density on  $y_+$  is highly nontrivial. However, the energy per unit length is a periodic function of  $y_+$ . Only for some special cases, like  $k_1 = k_2$  etc. the energy per unit length is constant and so does not depend on  $y_+$ . The time dependence of the energy density for all three solutions is shown in Fig. 10. The energy density for the mixed solution for  $x^3 = 0$  and  $x_0 = \pi/4$ ,  $x_0 = \pi$ ,  $x_0 = 7\pi/4$  is plotted in Fig. 11. For the case  $x^0 = \pi$  the peaks are maximally separated (this is not very clear without a detailed study of some other values  $x^0$ ). In this case the energy takes its maximal value, see Fig. 10.

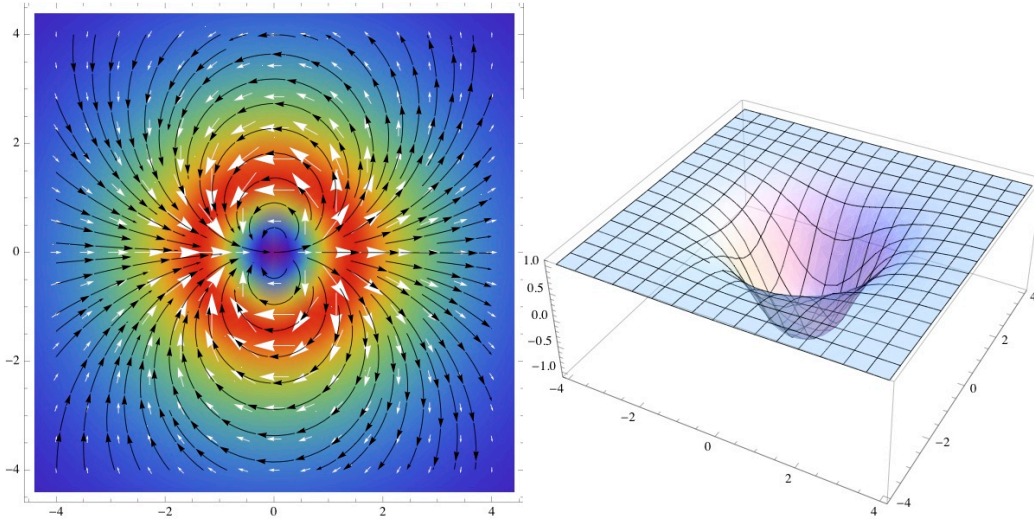


Figure 1: The tube solution. The part  $(n^1, n^2)$  (left) and the component  $n^3$  (right) of the isovector  $\vec{n}$  for  $a_1 = 0, a_2 = 0, a_3 = 2, x^0 = 0, x^3 = 0$  and  $k_2 = 2$ . The minimal value  $n^3 = -1$  occurs at the point  $x^1 = 0$  and  $x^2 = 0$ .

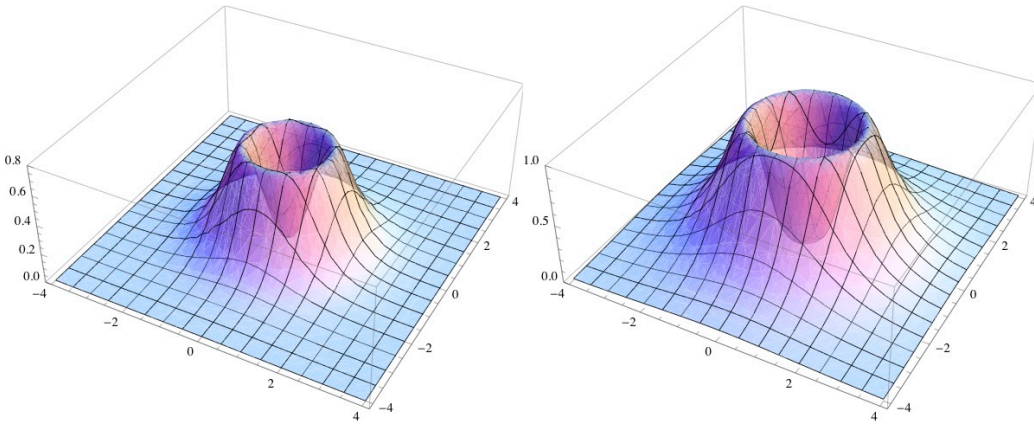


Figure 2: The energy density of the tube solution - the topological part (left) and the wave part (right). Here  $a_1 = 0, a_2 = 0, a_3 = 2, x^0 = 0, x^3 = 0$  and  $k_2 = 2$ .



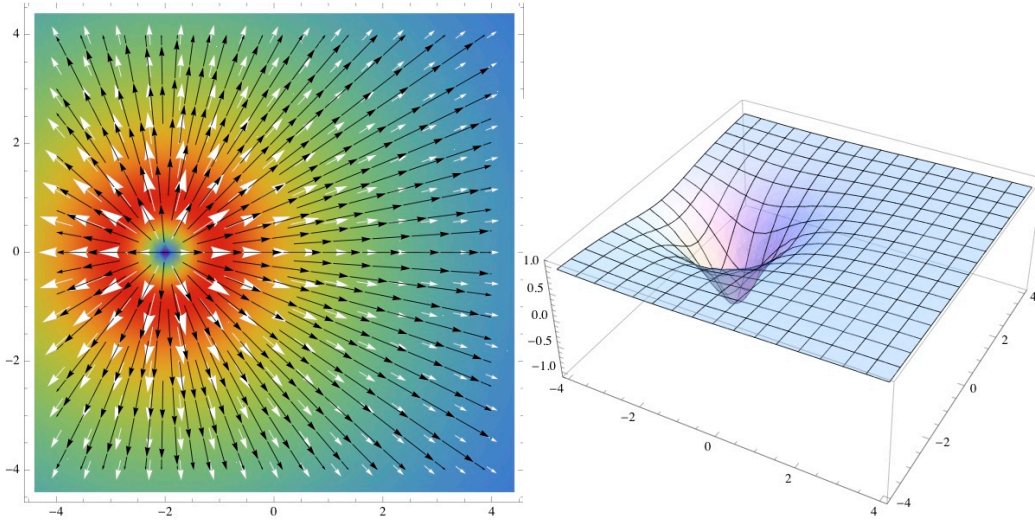


Figure 3: The spiral solution. The part  $(n^1, n^2)$  (left) and the component  $n^3$  (right) of the isovector  $\vec{n}$  for  $a_1 = 2$ ,  $a_2 = 1$ ,  $a_3 = 0$ ,  $x^0 = 0$ ,  $x^3 = 0$  and  $k_1 = 1$ . The minimal value  $n^3 = -1$  occurs at the point  $x^1 = -a_1 \cos(k_1 y_+)$  and  $x^2 = -a_1 \sin(k_1 y_+)$ ; here  $x^1 = -2$ ,  $x^2 = 0$ .

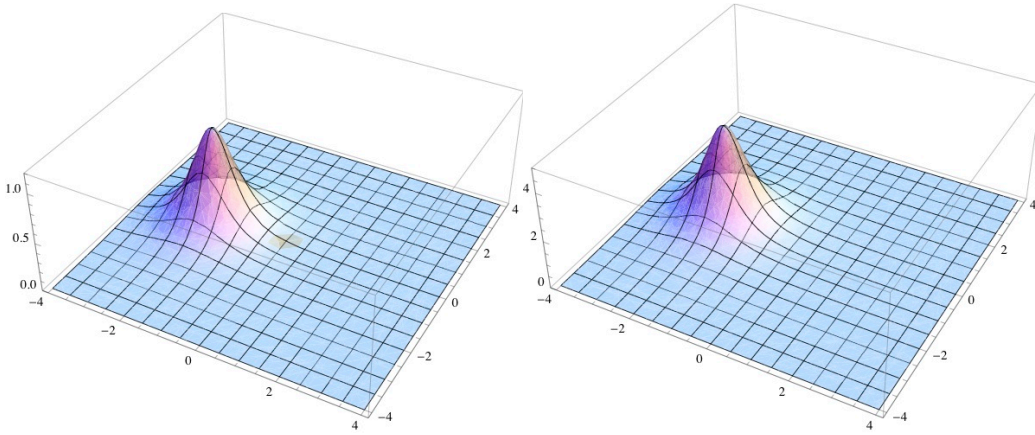


Figure 4: The energy density of the spiral solution - the topological part (left) and the wave part (right). Here  $a_1 = 2$ ,  $a_2 = 1$ ,  $a_3 = 0$ , and  $x^0 = 0$ ,  $x^3 = 0$  and  $k_1 = 1$ . The maxima of the energy density for both contributions are located at the same point on the plane  $x^1 x^2$  corresponding with the minimum of  $n^3$  (see Fig 3); here  $x^1 = -2$ ,  $x^2 = 0$ .

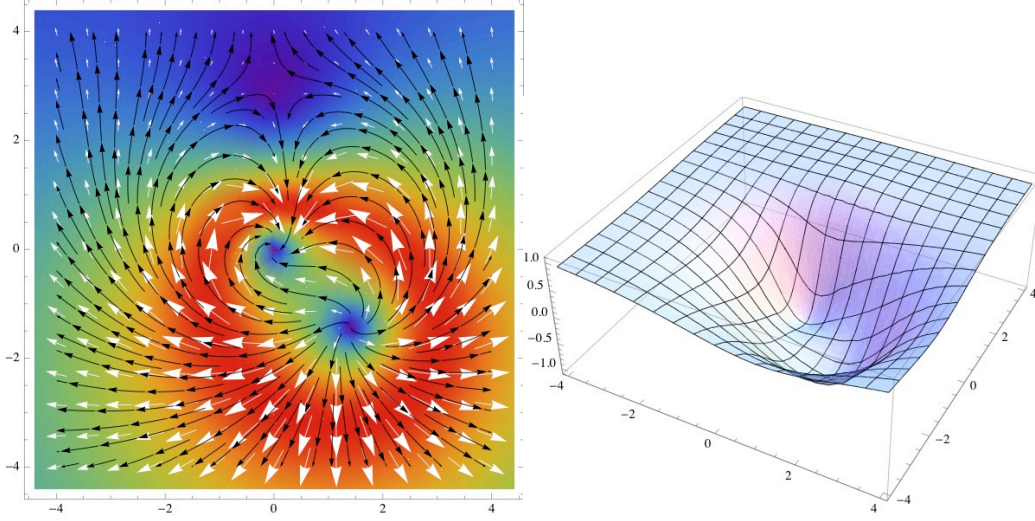


Figure 5: The  $CP^1$  solution with all  $a_k \neq 0$ . The part  $(n^1, n^2)$  (left) and the component  $n^3$  (right) of isovector  $\vec{n}$  for  $a_1 = 2$ ,  $a_2 = 1$ ,  $a_3 = 3$ ,  $x^0 = 3\pi/4$ ,  $x^3 = 0$ ,  $k_1 = 1$  and  $k_2 = 2$ .

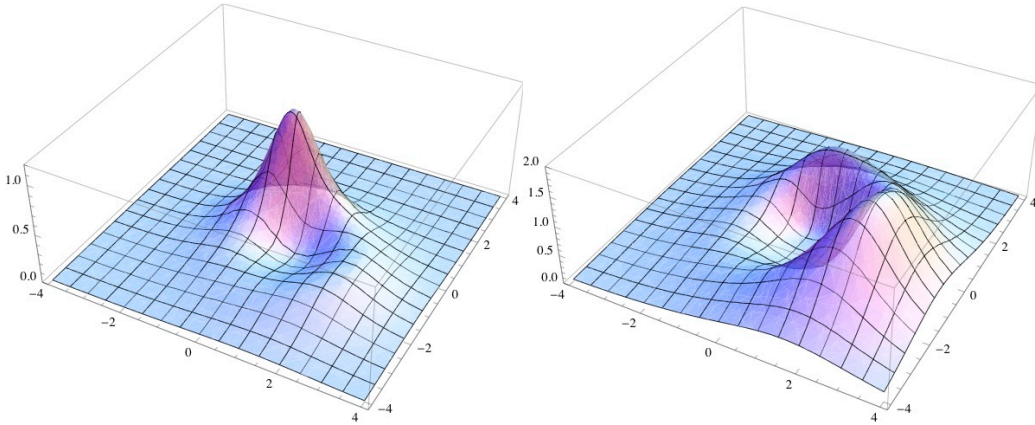


Figure 6: The energy density of the  $CP^1$  solution with all  $a_k \neq 0$  - the topological part (left) and the wave part (right). Here  $a_1 = 2$ ,  $a_2 = 1$ ,  $a_3 = 3$ ,  $x^0 = 3\pi/4$ ,  $x^3 = 0$ ,  $k_1 = 1$  and  $k_2 = 2$ .

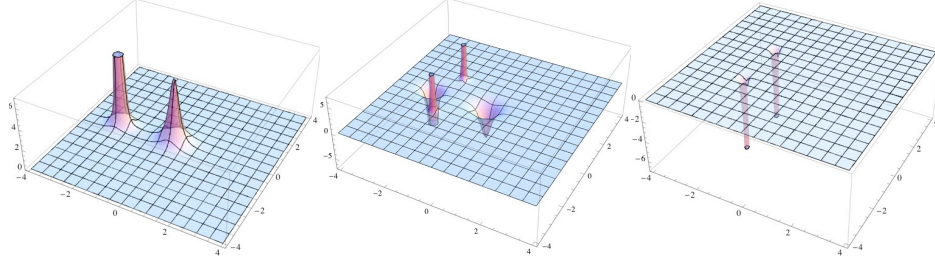


Figure 7: The functions  $\pi\rho_{\text{top}}$  (where  $\rho_{\text{top}}$  is a topological charge density) for  $x^0 = 0$ ,  $x^3 = 0$ ,  $a_1 = 2.5$ ,  $a_2 = 0.6$ ,  $a_3 = 1.0$ ,  $a_4 = 0.01$ ,  $k_1 = 1$  and  $k_2 = 2$ . The left picture corresponds to the holomorphic solution, the central picture corresponds to the mixed solution and the right picture to the anti-holomorphic solution.

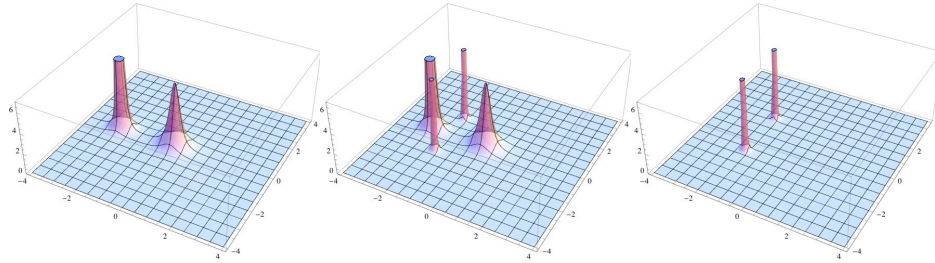


Figure 8: The functions  $\mathcal{H}^{(1)}/8M^2$  (proportional to topological contribution to the energy density) for  $x^0 = 0$ ,  $x^3 = 0$ ,  $a_1 = 2.5$ ,  $a_2 = 0.6$ ,  $a_3 = 1.0$ ,  $a_4 = 0.01$ ,  $k_1 = 1$  and  $k_2 = 2$ . The left picture corresponds to the holomorphic solution, the central picture corresponds to the mixed solution and the right picture to the anti-holomorphic solution.

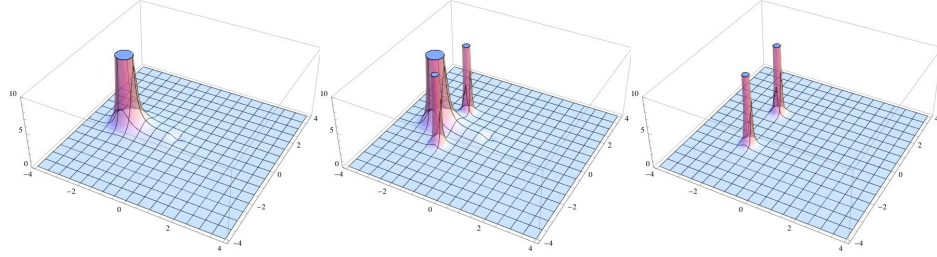


Figure 9: The functions  $\mathcal{H}^{(2)}/8M^2$  (proportional to wave contribution to the energy density) for  $x^0 = 0$ ,  $x^3 = 0$ ,  $a_1 = 2.5$ ,  $a_2 = 0.6$ ,  $a_3 = 1.0$ ,  $a_4 = 0.01$ ,  $k_1 = 1$  and  $k_2 = 2$ . The left picture corresponds to the holomorphic solution, the central picture corresponds to the mixed solution and the right picture to the anti-holomorphic solution.

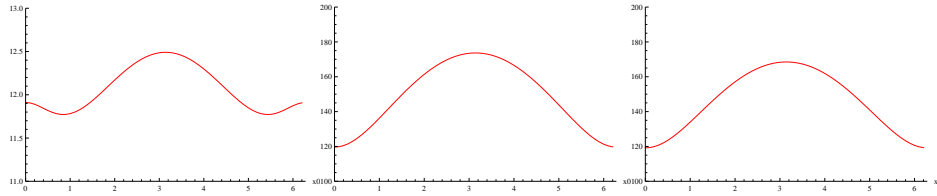


Figure 10: The integral  $\mathcal{I}^{(2)}$  as the function of  $x^0 \in [0, 2\pi]$ . The other parameters read:  $x^3 = 0$ ,  $a_1 = 2.5$ ,  $a_2 = 0.6$ ,  $a_3 = 1.0$ ,  $a_4 = 0.01$ ,  $k_1 = 1$  and  $k_2 = 2$ . The left picture corresponds to the holomorphic solution, the central picture corresponds to the mixed solution and the right picture to the anti-holomorphic solution.

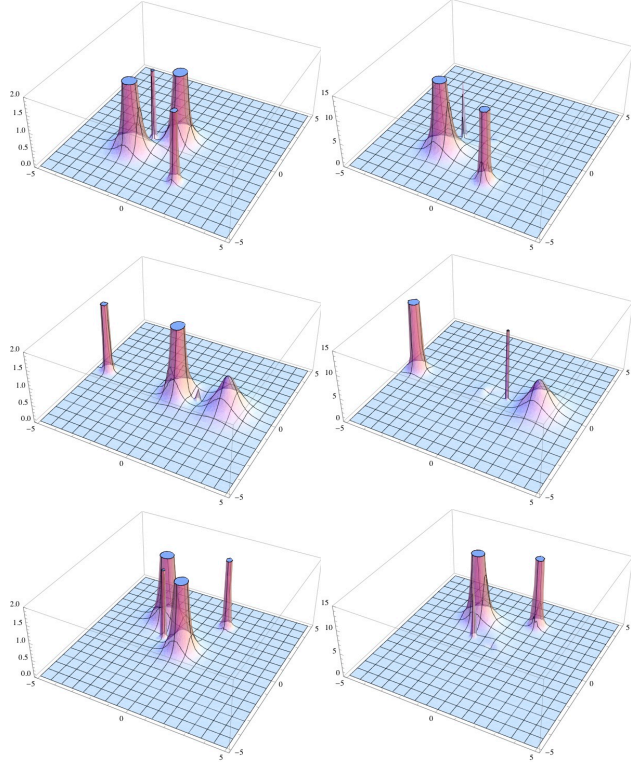


Figure 11: Time evolution of the mixed solution for  $a_1 = 2.5$ ,  $a_2 = 0.6$ ,  $a_3 = 1.0$ ,  $a_4 = 0.01$ ,  $k_1 = 1$  and  $k_2 = 2$ . The functions  $\mathcal{H}^{(1)}/8M^2$  (left column) and  $\mathcal{H}^{(2)}/8M^2$  (right column) have been considered for  $x^3 = 0$  at the moments  $x^0 = \pi/4$  (first row),  $x^0 = \pi$  (second row),  $x^0 = 7\pi/4$  (third row). Their values for  $x^0 = 0$  are sketched at the central pictures of Fig 8 and Fig 9.

## 5 Conclusions and Further Comments

In this paper we have demonstrated that the  $CP^N$  model in (3+1) dimensions has many classical solutions. Our construction has been based on the observation that one can generalise ideas used in the construction of solutions of the  $CP^N$  model in (2+0) dimensions and generate vortex and vortex-antivortex like solutions of this model in (3+1) dimensions. Like for the model in (2+0) dimensions we can generate these solutions from field configurations described by polynomial functions of  $x^1 + i\epsilon_1 x^2$ . This time the coefficients of these functions could be also functions of  $x^3 + \epsilon_2 x_0$ . The energy of such configurations is infinite (as the energy density is independent of  $x^3$ ) and so we interpret these solutions as describing systems of vortices and antivortices.

Of course our expressions solve equations in (3+1) dimensions and they also determine the dynamics of these vortices.

In this paper we have only looked at the simplest solutions (corresponding to very few vortices) with the time dependence being described by simple phase factors. Even in this case the observed dynamics is quite complicated and has exhibited various interesting properties. In particular, we have shown that the vortices can rotate in space (physical and internal) and their energy per unit length of the vortex can vary in time. During this time evolution some vortices can shrink to delta functions and then expand again often being characterised by a very periodical behaviour.

One other unusual property is their dependence on the distance between the vortices: the energy density of two vortices can depend on the distance between them and can possess a minimum at a specific value of this distance. This suggests that vortices which are located at non-minimal distances may be unstable and so could try to reduce their energy per unit length by moving towards this optimal configurations. However, their configurations are solutions for any distance as their infinite ‘inertia’ stops them from moving towards each other without an external push.

We are now looking at other properties of these and other solutions.

**Acknowledgment:** L.A. Ferreira and W.J. Zakrzewski would like to thank the Royal Society (UK) for a grant that helped them in carrying out this work. L.A. Ferreira is partially supported by CNPq (Brazil) and P. Klimas is supported by FAPESP (Brazil).

## References

- [1] A. D'Adda, P. Di Vecchia and M. Luscher, *A  $1/N$  expandable series of non-linear  $\sigma$  models with instantons*, Nucl. Phys. B 146, (1978), 63
- [2] W.J. Zakrzewski, *Low Dimensional Sigma Models* (Hilger, Bristol, 1989).
- [3] L. A. Ferreira, P. Klimas and W.J. Zakrzewski, *Some  $(3+1)$ -dimensional vortex solutions of the  $CP^N$  model*, Phys. Rev. **D 83** (2011) 105018
- [4] L. A. Ferreira, *Exact vortex solutions in an extended Skyrme-Faddeev model*, JHEP **05** (2009) 001 [arXiv: 0809.4303]
- [5] L. A. Ferreira, P. Klimas, *Exact vortex solutions in a  $CP^N$  Skyrme-Faddeev type model*, JHEP **10** (2010) 008 [arXiv: 1007.1667]
- [6] N. Manton and P.M. Sutcliffe , *Topological Solitons*, Cambridge University Press, Cambridge U.K. (2004).